ACS APPLIED MATERIALS & INTERFACES

Research Article

www.acsami.org

Optical Properties of Water-Soluble CdTe Quantum Dots Passivated by a Biopolymer Based on Poly((2-dimethylaminoethyl) methacrylate) Grafted onto κ-Carrageenan

Ghasem Rezanejade Bardajee,*,† Zari Hooshyar, Habib Rezanezhad,‡ and Gerald Guerin§

†Department of Chemistry, Payame Noor University, PO BOX 19395-3697, Tehran, Iran

‡Department of Biology, Faculty of Science, Ferdowsi University, Mashhad, Iran

§Department of Chemistry, University of Toronto, 80 St. George Street, Toronto, Canada M5S 3H6

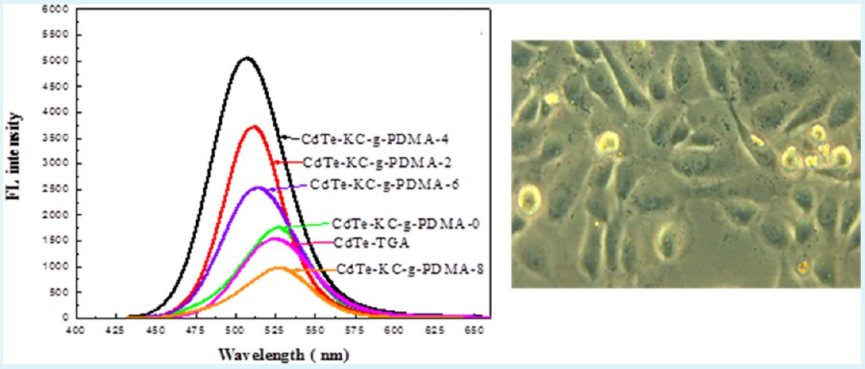

ABSTRACT: Poly ((2-dimethylaminoethyl) methacrylate) grafted onto κ-carrageenan (κC-g-PDMA) as a biopolymer was synthesized and applied for surface modification of water-soluble CdTe quantum dots (QDs). The effects of DMA concentration, molar ratio of κC-g-PDMA/CdTe, reaction temperature and time on optical properties of CdTe QDs were investigated via fluorescent (FL) and UV- visible spectra. The results showed that the κC-g-PDMA significantly affects the optical properties of CdTe QDs. The obtained samples were characterized by Fourier transform infrared spectrum (FT-IR), thermogravimetric (TG) analysis, and transmission electron microscopy (TEM). The antibacterial activity, antifungal assays, and cytotoxicity of modified QDs were examined, and a good biocompatibility was observed.

KEYWORDS: *optical properties, biopolymer, CdTe quantum dots, water-soluble, cytotoxicity*

1. INTRODUCTION

CdTe quantum dots (QDs) are nanoparticles from group II−VI elements in size range of 1−10 nm. They have many unique electronic and optical properties, such as large absorption cross-section, good chemical and photostability, size dependent emission wavelength tunability, and narrow emission peak width at half height.[1−6] Because of these features, they have been extensively studied for practical applications, such as solar cells,[7] optoelectronic transistor components,[8] and fluorescent (FL) biological labels,[9] in the past few decades.

Generally, two synthetic routes, that is, organic-phase and aqueous-phase approaches, to produce CdTe QDs with desired optical properties have been proposed. Organometallic based reactions have been used for the synthesis of CdTe QDs in organic-phase. These QDs have a capping layer composed of one or more organic ligands such as trioctylphosphine[10] or trioctylphosphine oxide, fatty acids,[11] and alkyl amines.[12] Although CdTe QDs synthesized in the organic phase are highly fluorescence, they are not compatible with the biological system. In contrast, in aqueous-phase approache, CdTe QDs are directly prepared in water using some water-soluble thiol-containing molecules such as mercaptoacetic acid[13] and thioglycolic acid.[14] Although these thiol capping agents are reagent-effective and less toxic, they have low FL intensity and poor stability, limiting their applications. To overcome these drawbacks, several strategies such as high temperature and high pressure have been utilized to produce CdTe QDs with higher FL intensities.[15−19]

In the present study, we investigate the FL properties of CdTe QDs surrounded by a natural water-soluble multidentate biopolymer based on poly ((2-dimethylaminoethyl) methacrylate) grafted onto κ-carrageenan (κC-g-PDMA). κC is a sulfated polysaccharide and belongs to the large family of carrageenans which are extracted from red seaweeds.[20−22] κC contains both sulfated and nonsulfated repeating galactose units and 3, 6 anhydrogalactose (3, 6-AG), connected together by alternating alpha 1−3 and beta 1−4 glycosidic linkages (Figure 1). Due to their excellent physical functional properties and biological activities, κC is extensively utilized in the food, cosmetics, textile,

Received: April 6, 2012
Accepted: June 26, 2012
Published: June 26, 2012

   dx.doi.org/10.1021/am300566u | ACS Appl. Mater. Interfaces 2012, 4, 3517−3525

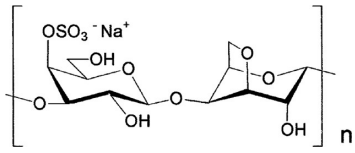

Figure 1. General structure of κC units.

and pharmaceutical industries.[23−25] Our experimental results clearly give the evidence of beneficial influence of κC-g-PDMA on FL intensity and quantum yield of CdTe QDs. The effective factors and optimum conditions of the ligand exchange have been investigated and based on these results; the reasons of FL intensity enhancement have been hypothesized. To evaluate the effect of surface modified QDs on mammalian cells, the MTT assay was performed and almost no cytotoxicity was observed.

2. EXPERIMENTAL SECTION

2.1. Materials. κC was obtained from Condinson, Denmark. DMA (98%), thioglycolic acid (TGA, 98%), $CdCl_2 \cdot 5H_2O$ (99.99%), tellurium (Te) powder (99.997%), and sodium borohydride ($NaBH_4$, 95%) were purchased from Sigma−Aldrich. Ammonium persulfate (APS, 99%) was obtained from Fluka and used without further purification. Other chemicals and solvents were analytical grade and purchased from LOBA chemicals (India). Gram-negative *Escherichia coli* (*E. coli* ATCC 51813) and gram-positive *Bacillus licheniformis* (*B. licheniformis* ATCC 12759) bacteria were prepared from NIGEB Bacterial Bank (Tehran, Iran). *Sclerotinia Sclerotiorum* (*S. sclerotiorum*) fungus was purchased from NIGEB Fungi Bank (Tehran, Iran). Luria−Bertani (LB) agar powder was purchased from Sigma (MBA, Sigma Chemical Co., St. Louis, MO). The human bladder epithelial cell line HTB 5637 (ATCC HTB-9) was grown in RPMI 1640 (Invitrogen) supplemented with 10% fetal bovine serum (HyClone, Logan, UT). Double distilled water was used to prepare the solutions.

2.2. Apparatus. FT-IR spectra of samples in the form of KBr pellets were recorded using a Jasco 4200 FTIR spectrophotometer. A Shimadzu UV−vis 1650 PC spectrophotometer was used for recording absorption spectra in solution. FL spectra were measured using SCINCO's Fluorescence Spectrometer FluoroMate FS-2. All samples were placed in a 1.00 cm quartz cuvette either for UV or fluorescence measurements. The dynamic weight loss tests were conducted on a TA Instruments 2050 thermogravimetric (TG) analyzer. All tests were conducted under N_2 atmosphere (25 mL/min) using sample weights of 5−10 mg over a temperature range of 25−600 °C at a scan rate of 20 °C/min. The mass of the sample pan was continuously recorded as a function of temperature. Transmission electron microscopy (TEM) was taken on a Zeiss TEM at an acceleration voltage of 80 kV. Samples for TEM were prepared by putting a drop of solution on a carbon-coated copper grid. MTT test was performed by multichannel photometer (Labsystem MS, Finland) apparatus in 580 nm filter.

2.3. Synthesis of CdTe-TGA QDs. NaHTe was prepared according to the previously reported procedure.[14−16] First of all, 0.025 g of tellurium powder and 2.5 mL of ultrapure water were added to a small flask. Then 0.025 g of sodium borohydride was added in the flask. After about 2 h, the black tellurium powder disappeared and NaHTe was produced. Then, NaHTe was added to cadmium chloride solution in the presence of TGA under N_2 atmosphere with a molar ratio of Cd^{2+}/Te^{2-}/TGA fixed at 1:0.5:2.4. After it was mixed, the solution was heated to 100 °C for 1 h, leading to the preparation of CdTe-TGA QDs (Scheme 1).

2.4. Synthesis of κC-g-PDMA. κC-g-PDMA was prepared according to our previously reported procedure.[26−28] Typically, different amounts of DMA monomers (0, 2, 4, 6, and 8 mL (0−42 mmol)) were dissolved in a three-neck reactor containing a homogeneous mixture of κC (1.0 g) and water (80 mL). Then, APS (0.09 g (0.4 mmol)) in H_2O (5.0 mL) was added while the temperature of the reactor was controlled by a thermo-stated water bath at 80 °C, as shown in Scheme 2. After 30 min stirring, the formed viscous solution was dewatered by ethanol (200 mL) to remove unreacted monomers and homopolymers. In the following text, all κC-g-PDMA will be marked by amount of DMA monomer in mL. For instance, κC-g-PDMA-4 means a graft copolymer sample which is prepared by mixing 4 mL of DMA with 1.0 g of κC.

2.5. Preparation of CdTe- κC-g-PDMA QDs. The synthesized CdTe-TGA QDs was added to the viscous solution of κC-g-PDMA-0 (i.e., pure κC), κC-g-PDMA-2, κC-g-PDMA-4, κC-g-PDMA-6, and κC-g-PDMA-8 biopolymers in same conditions. The solutions were stirred for 60 min at room temperature to ensure distribution of the CdTe QDs into the biopolymer chains. Meanwhile, the optical properties of the solution were studied via UV−vis and fluorescence measurements at different time intervals. After that, ethanol was added to the solution, centrifuged and the residue was collected for further experiments.

2.6. Biocompatibility. Antibacterial assays were done against gram-negative *E. coli* and gram-positive *B. licheniformis* bacteria by disk diffusion method. The bacteria were grown on a LB broth/agar medium at 37 °C for 16−19 h. Antifungal assay was performed against S. Sclerotiorum fungus by disk diffusion technique. Potato dextrose agar (PDA) medium was used to cultivate the fungus at 30 °C for 48 h. To evaluate the effect of CdTe-κC-g-PDMA QDs on mammalian cells, the MTT assay was performed.

3. RESULTS AND DISCUSSION

Our experiments showed that the optical properties of CdTe-κC-g-PDMA QDs depend on various factors, such as concentration of DMA monomer, molar ratio of kC-g-PDMA/CdTe, and reaction temperature. Thus the preparation strategy needs careful manipulation of experimental conditions to generate high FL intensity from CdTe- κC-g-PDMA QDs.

3.1. Effect of DMA Concentration. To study the effect of DMA concentration on optical properties of CdTe-κC-g-PDMA QDs, the FL and absorption spectra of CdTe-κC-g-PDMA-0 (i.e., CdTe-κC), CdTe-κC-g-PDMA-2, CdTe-κC-g-PDMA-4, CdTe-κC-g-PDMA-6, and CdTe-κC-g-PDMA-8 were investigated. Figure 2 depicts the FL and UV−vis spectra of these samples. As shown in Figure 2a, the FL intensity initially increased with increasing monomer concentration up to 4 mL and then decreased with further increase in monomer amount.

Scheme 1. Synthesis of CdTe-TGA QDs

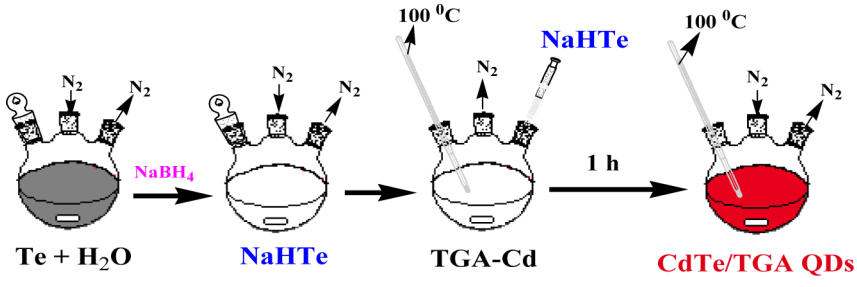

Scheme 2. General Route for the Synthesis of κC-g-PDMA

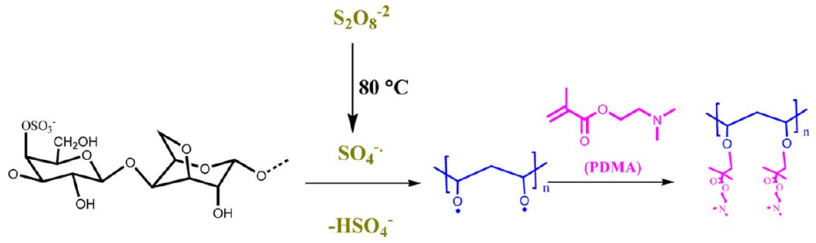

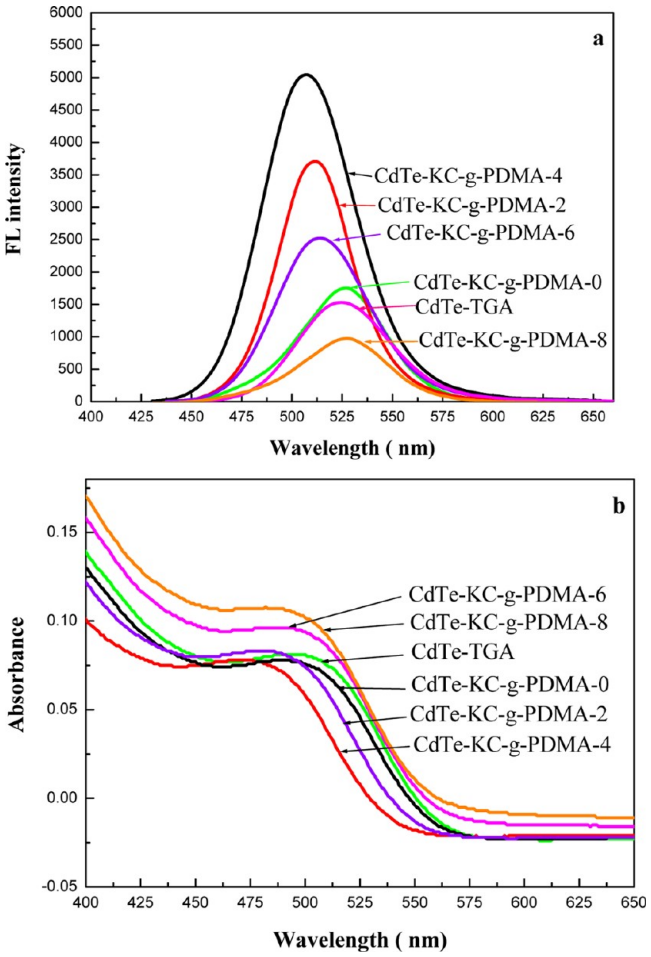

Figure 2. Comparison of (a) FL, and (b) absorption spectra of CdTe-κC-g-PDMA-0, CdTe-κC-g-PDMA-2, CdTe-κC-g-PDMA-4, CdTe-κC-g-PDMA-6, and CdTe-κC-g-PDMA-8 after 1 h stirring at 25 °C (λ_{ex} for emission spectra = 380 nm and all other conditions were kept the same.

The initial increase in FL intensity can be attributed to an increase in the quantity of dimethylamino chelating groups (from PDMA) on the polysaccharide backbones (containing hydroxyl functional groups) which would enhance the passivation of QDs in the water. The subsequent decrease of FL intensity at higher amounts of DMA in the graft copolymer may be attributed to an increase in viscosity of the medium that hinders the effective movement of the QDs and polymer chains to decrease efficient interaction between them. In addition, FL peak positions of CdTe QDs in these samples are changed. This phenomenon is related to size changing of CdTe QDs in biopolymer. According to known theory of quantum size effects, with decreasing size, the emission maximum can shift to higher energies (blue shift). The size of CdTe QDs in these samples can be determined by the first excitonic absorption peak according to eq 1.[29]

$$D = (9.8127 \times 10^{-7})\lambda^3 - (1.7147 \times 10^{-3})\lambda^2 + (1.0064)\lambda - 194.84 \quad (1)$$

The particle sizes of CdTe QDs was around 2.5, 1.9, 1.5, 2.2, and 2.3 nm, corresponding with CdTe-κC-g-PDMA-0, CdTe-κC-g-PDMA-2, CdTe-κC-g-PDMA-4, CdTe-κC-g-PDMA-6, and CdTe-κC-g-PDMA-8 samples, respectively. The ligand exchange usually accompanies with a small blue shift in the band-edge absorption and a small reduction in particle size. From these results, we infer that the TGA ligands are removed from the surface of the CdTe QDs and replaced by κC-g-PDMA biopolymers. This ligand exchange induces an etching of the surface of the QDs which in this case led to the shift of excitonic absorbance peak to lower value.[30] The size of QDs decreases with increasing the amount of PDMA in the κC-g-PDMA from 0 to 4 and then increases for larger value of PDMA in the κC-g-PDMA. Similarly, one observes that the first exitonic absorbance peak and the wavelength at the maximum fluorescence intensity decrease when the ratio is increases from 0 to 4 prior to a decrement for higher ratios. The ligand exchange can etch the surface of QDs and reduce the size of QDs. More efficient ligand exchange (from κC-g-PDMA-0 to κC-g-PDMA-4) can lead to a better etching and consequently smaller sizes. After that (for κC-g-PDMA-6 and κC-g-PDMA-8), the aggregation of QDs in same chains can lead to an apparent increase of their size.

Due to the highest FL intensity obtained with CdTe-κC-g-PDMA-4 QDs, we focused on further study of this sample.

3.2. Effect of Molar Ratio of κC-g-PDMA-4: CdTe on FL Properties. The molar ratio of κC-g-PDMA-4/CdTe is another important factor that strongly influences the optical properties of CdTe-κC-g-PDMA-4. To observe the ratio effect of κC-g-PDMA-4/CdTe on FL properties, we changed the amount of κC-g-PDMA-4, while the other parameters, such as amount of CdTe-TGA QDs and temperature, were fixed. Figure 3 shows the influence of the ratio of κC-g-PDMA-4/CdTe on the FL intensity and the first excitonic absorption peak of CdTe-κC-g-PDMA-4QDs. As one can see in Figure 3, the FL intensity of QDs is increased by increasing the κC-g-PDMA-4/CdTe ratio up from 1:1 to 4:1. At the same time, the first excitonic absorption peak of QDs shifts to lower wavelengths. However, in higher ratios of κC-g-PDMA-4/CdTe (larger than 4:1), the FL intensity and the position of the absorption peaks remain constant. These characteristics for ratios higher than 4:1, can be attributed to the uniform distribution of CdTe QDs on the kC-g-PDMA-4 biopolymer support in the solution.

3.3. Effect of Reaction Temperature. To examine the effect of the reaction temperature on the optical properties of the CdTe-κC-g-PDMA-4, we kept all other experimental variables constant and changed the reaction temperature from 10 and 25

dx.doi.org/10.1021/am300566u | ACS Appl. Mater. Interfaces 2012, 4, 3517−3525

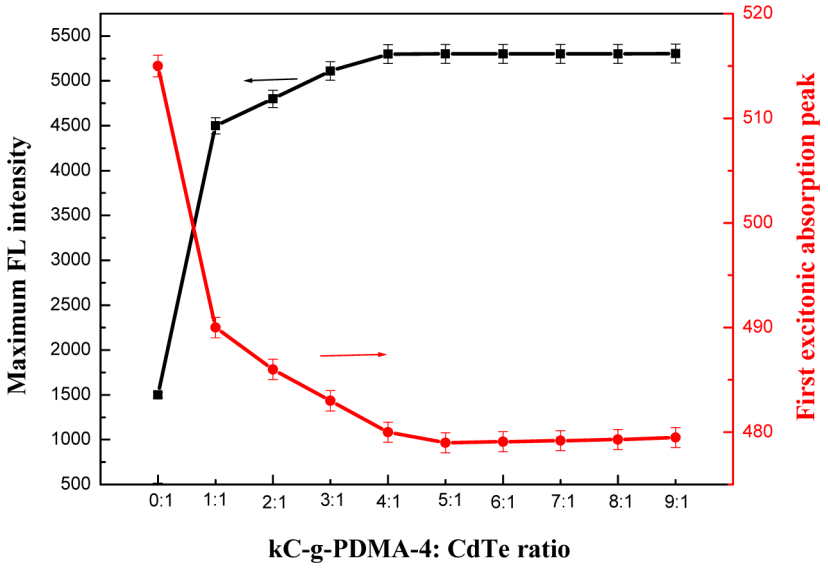

Figure 3. Comparison of maximum FL intensity and first excitonic absorption peak of CdTe-κC-g-PDMA-4, depending on the κC-g-PDMA-4/CdTe ratio, after 1 h stirring at 25 °C (λ_{ex} for emission spectra = 380 nm and all other conditions were kept the same).

to 50, 75, and 100 °C. Figure 4a shows the effect of reaction temperature on the FL intensity of the CdTe-κC-g-PDMA-4. A steady decrease in the FL intensity of CdTe QDs with the increase of reaction temperature was observed. This decrease indicates that the rate of the polymeric shell deposition is faster at higher temperatures. Furthermore, the absorption spectra under different temperatures are given in Figure 4b. As one can see in Figure 4b, there is a slight red shift in the absorption spectra with increasing temperature. This demonstrates that the smallest size of CdTe QDs is obtained at 25 °C. Nevertheless, it is worth noting that the reaction is facile at room temperature with highest FL intensity and smallest size of CdTe QDs.

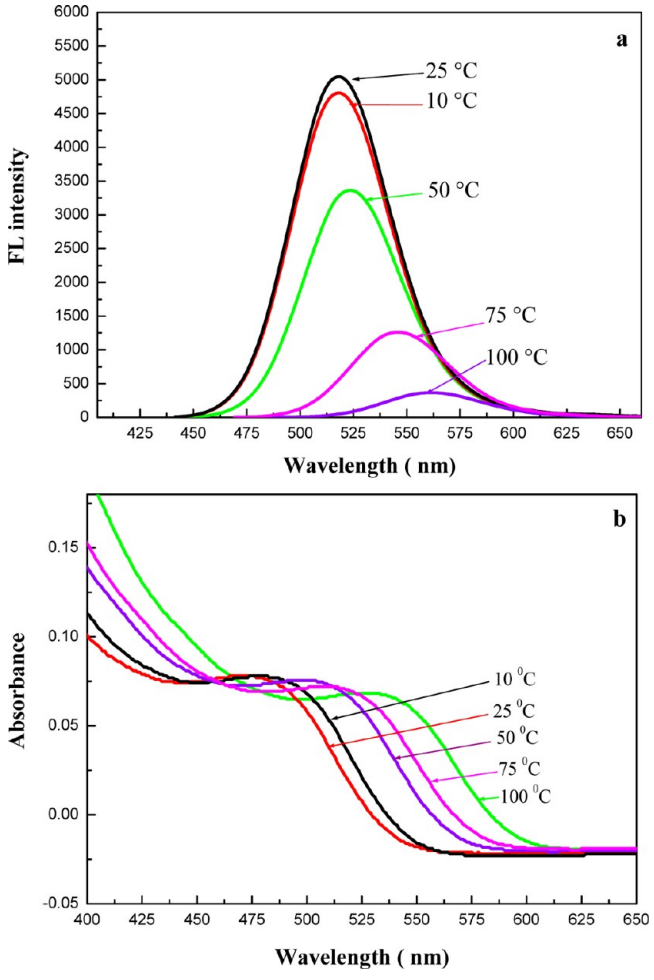

Figure 4. Comparison of (a) FL intensity and (b) UV spectra of CdTe-κC-g-PDMA-4 QDs at different temperatures after 1 h stirring (λ_{ex} for emission spectra = 380 nm and CdTe/κC-g-PDMA-4 = 1:4.

3.4. Effect of Stirring Time. The effect of stirring time on the FL intensity of CdTe-κC-g-PDMA-4 was also studied and the results are shown in Figure 5. This kinetic study revealed that the FL intensity of CdTe-κC-g-PDMA-4 initially increased with stirring time before to reach a plateau value for stirring times larger than 60 min. This experiment shows the minimum time for the anchoring of biopolymer ligands on the surface of QDs.

3.5. Investigation on Aging at Ambient Conditions. In Figure 6, the effects of aging on the FL properties of CdTe-κC-g-

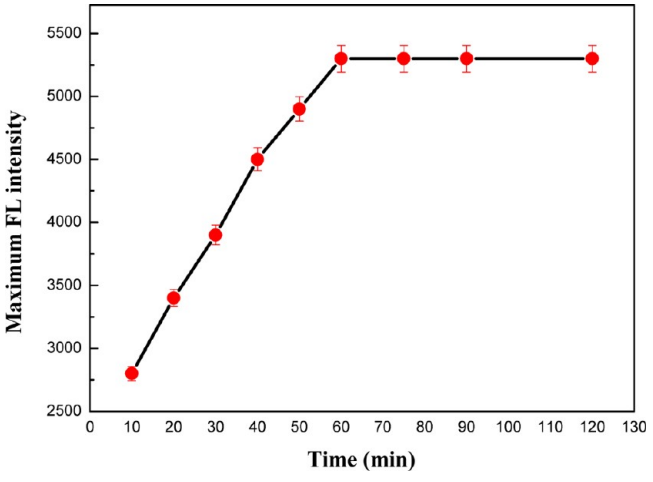

Figure 5. FL spectra of CdTe-κC-g-PDMA-4 QDs at different stirring times (λ_{ex} for emission spectra =380 nm and CdTe/κC-g-PDMA-4 = 1:4) at 25 °C (all other conditions were kept the same.

dx.doi.org/10.1021/am300566u | ACS Appl. Mater. Interfaces 2012, 4, 3517−3525

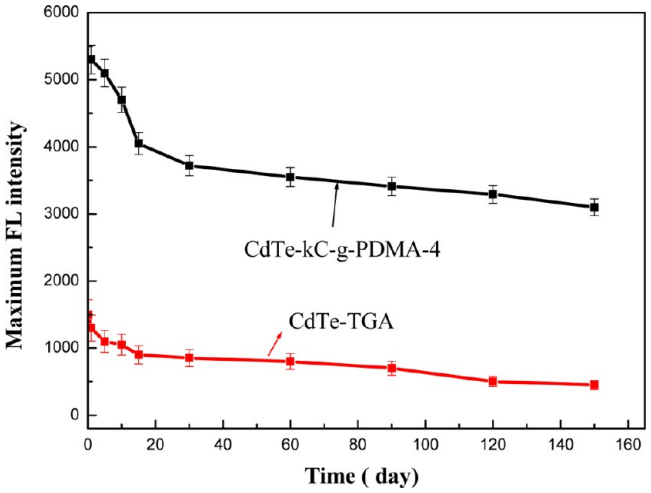

Figure 6. Comparison of FL spectra of CdTe-TGA and CdTe-κC-g-PDMA-4 QDs (CdTe/κC-g-PDMA-4 = 1:4) at different time intervals (λ_{ex} for emission spectra = 380 nm and CdTe/κC-g-PDMA-4 = 1:4) at 25 °C.

PDMA-4 QDs and CdTe-TGA QDs are demonstrated. From Figure 6, the FL intensity of the CdTe-TGA and CdTe-κC-g-PDMA-4 QDs are slowly decreased and became almost constant after 90 days. Furthermore, the aggregation of CdTe-TGA QDs was observed after 7 days aging at room temperature. This slower aging for modified QDs is directly linked to the presence of κC-g-PDMA-4 biopolymer around the QDs which causes a higher stability.

3.6. Characterization of CdTe-κC-g-PDMA-4 QDs. To verify that the TGA ligands have been removed from the surface of CdTe QDs, we performed FT-IR of the QDs before and after ligand exchange to characterize the functional groups present on the surface of CdTe QDs. Figure 7 depicts the FT-IR spectra of κC, κC-g-PDMA-4, CdTe-κC-g-PDMA-4, and CdTe-TGA QDs. In the spectrum of κC (Figure 7a), characteristic peaks, namely, stretching vibration bands at 841, 912, 1016, 1220, and 3300 cm^{-1} can be attributed to D-galactose-4-sulfate, 3,6-anhydro-D-galactose, glycosidic linkage, ester sulfate and hydroxyl groups of κC, respectively. As one can see in Figure 7a and b, the spectrum of κC-g-PDMA-4 represents the characteristic absorptions of κC and PDMA. The κC-g-PDMA-4 (Figure 7b) showed additional absorption peaks at 1660 cm^{-1} and 1465 cm^{-1} relating to C═O and C−O stretching vibrations of PDMA on the κC backbone. The broad peak observed at 3400 cm^{-1} is due to the stretching vibrations of OH functional groups in the polymer networks. The spectrum shown in Figure 7c (CdTe-κC-g-PDMA-4) is similar to the spectrum shown in Figure 7b. However one can observes in Figure 7c that some absorption peaks in Figure 7b have been slightly shifted. These shifts could be attributed to the chelation of the biopolymer functional groups on the surface of CdTe QDs. The absence of TGCA functional groups (Figure 7d) and specially thiols stretching vibrations at 2600 cm^{-1} after ligand exchange in Figure 7c can provide more evidence for replacement of TGCA by biopolymer residues.

Furthermore, the thermal decomposition behaviors of κC-g-PDMA-4 and CdTe-κC-g-PDMA-4 were evaluated to confirm the presence of CdTe QDs in κC-g-PDMA-4 matrix. The TG-DTG curves for κC-g-PDMA-4 and the CdTe-κC-g-PDMA-4 are shown in Figure 8a. As it is shown on the TG-DTG curves, CdTe QDs have a positive effect on the thermal decomposition of κC-g-PDMA-4. These results are confirmed by comparing the TG-DTA curve of CdTe-κC-g-PDMA-4 with the κC-g-PDMA-4 in Figure 8b. It can be explained by the catalytic effect of CdTe on the elimination of CO_2 from the polymeric chains. The weight loss difference between the CdTe-κC-g-PDMA-4 and κC-g-PDMA-4 at 550 °C can be applied for the measurement of CdTe QDS participation in the polymer matrix. Accordingly, the 7.9% of CdTe QDs was incorporated into κC-g-PDMA-4 biopolymer matrix.

Figure 9 shows TEM images of CdTe-κC-g-PDMA-4 and CdTe-TGA QDs. The TEM images and the related particle size histograms of obtained samples (Figure 9) suggest that the average size of CdTe QDs change from 2.8 to 1.7 when their surface are modified by κC-g-PDMA-4, which is in good

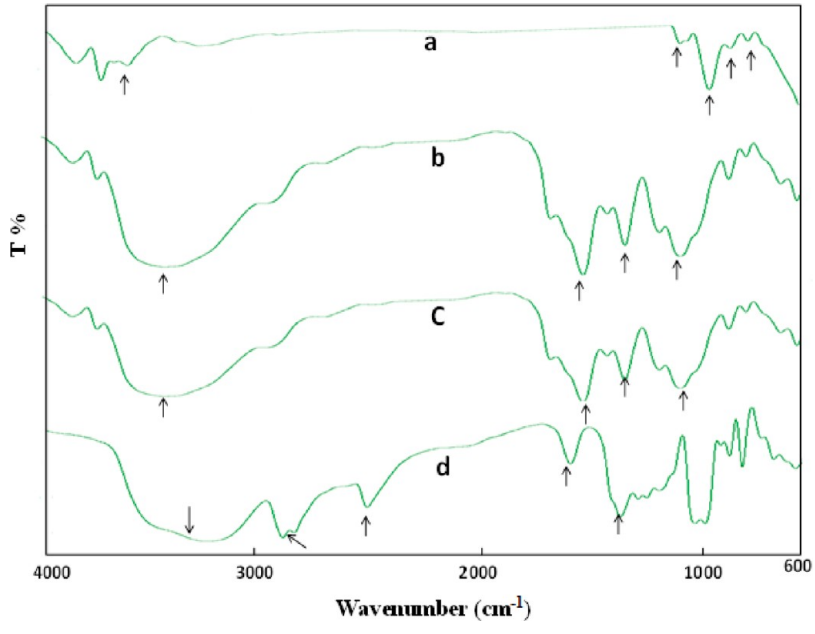

Figure 7. FT-IR spectra of (a) κC, (b) κC-g-PDMA-4, (c) CdTe-κC-g-PDMA-4, and (d) CdTe-TGA.

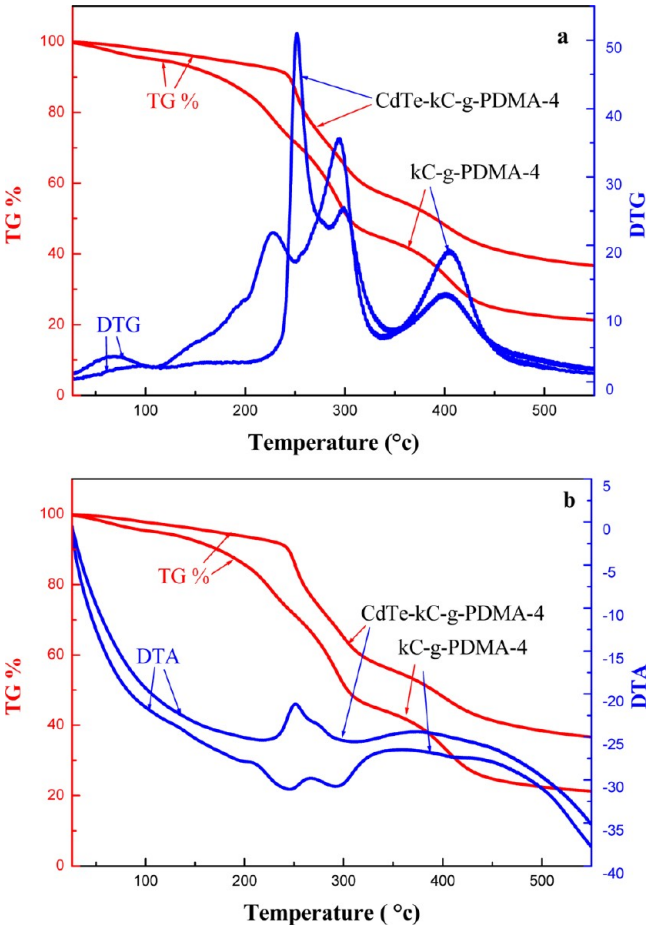

Figure 8. (a) TG/DTG and (b) TG/DTA curves of CdTe-κC-g-PDMA-4 and κC-g-PDMA-4.

agreement with the average particle size obtained using UV results.

Binding of κC-g-PDMA-4 to the surface of CdTe QDs can be further supported by thermodynamic rules. The driving force of this interaction may come from two effects: one is the entropic gain that derives from the dissociation of TGA ligands from the QD surfaces, assuming that the entropy loss from the polymer binding to QDs is much smaller. The other is the enthalpic effect from the binding between the functional groups of the polymer and the Cd sites on the QD surfaces.

The interaction of freshly prepared κC-g-PDMA with CdTe-TGA QDs can be considered as a very simple and straightforward method for the fabrication of CdTe- κC-g-PDMA QDs. It can be considered that the CdTe-TGA QDs when stirred with κC-g-PDMA, get well embedded in polymer chains through dimethylamino (from PDMA) functional groups via a ligand exchange process as shown in Scheme 3.

The quantum yield (QY) of CdTe-TGA and CdTe-κC-g-PDMA-4 QDs was measured according to the method described in the ref 31. Briefly, rhodamine 6G in water was chosen as a reference standard (QY = 0.90), and the absorbance for the standard and the QDs solutions at the excitation wavelengths in water was measured (6 different solutions for each sample with an absorbance at excitation wavelength around 0.1). The fluorescence spectra of each solution were measured and the integrated fluorescence intensity (that is, the area of the fluorescence spectrum) was calculated. The areas of the integrated fluorescence intensity vs absorbance were plotted. The plot obtained should be a straight line with a gradient (Grad), which was used to calculate the quantum yield based on the eq 2

$$\Phi_X = \Phi_{ST}(\mathrm{Grad}_X/\mathrm{Grad}_{ST})(\eta_X^2/\eta_{ST}^2) \quad (2)$$

Where the subscripts ST and X denote standard (rhodamine 6G) and test samples respectively, Φ is QY, and η is the refractive index of the solvent. The QY of the CdTe-TGA and CdTe-κC-g-PDMA-4 QDs was calculated 0.29 and 0.44, respectively. This result shows an increase in the QY of QDs after ligand exchange process with κC-g-PDMA-4 biopolymer.

3.7. Antibacterial Activity by Agar Diffusion Technique. To probe the antibacterial effects of CdTe-κC-g-PDMA-4 QDs against gram-negative *E. coli* and gram-positive B. Licheniformis bacteria, the effects have been evaluated by agar diffusion technique. The minimum inhibitory concentration (MIC) and the minimum bactericidal concentration (MBC) are the lowest concentrations (μg/mL) at which a compound can inhibit bacterium growth or kill more than 99% of the added bacteria, respectively. Figure 10 shows the typical antibacterial test results of CdTe-κC-g-PDMA-4 QDs by the disk diffusion method. In this test the zone of inhibition (ZoI), where no visible bacterial colonies formed, is measured by the diameter of the inhibition zone under and around the tested samples which was measured using a caliper. First the tested bacteria were cultivated on the surface of LB nutrient agar plates, then QDs samples were placed on the surface. After 24 h incubation at 37 °C, no *B. licheniformis* and *E. coli* bacteria colonies could grow around QDs samples on the LB agar plates. This clearly demonstrates that CdTe-κC-g-PDMA-4 QDs has excellent bacterial inhibition growth capabilities.

In another test, bacterial growth was evaluated by visual turbidity of the LB broth. LB broth without bacterial growth is clear and after growing the bacteria, the medium becomes turbid. At first 10^5−10^6 cfu/ml of tested bacterial added to 6 mL of LB medium in sterile falcon. Dilution of QDs was achieved by a series solution technique, so different concentrations (2.0, 5.0, 8.0, 10.0, and 12.0 μg/mL) were achieved and added to medium and were incubated at 37 °C for 24 h. After this time, the turbidity of cultures was monitored. The transparency of LB broth is related to the inhibition of bacterial growth (bacteriostatic) or killing bacterial completely (bactericidal). To determine the MIC and MBC, 100 μL aliquots from the incubated LB broth were taken and spread on nutrient agar plates and were incubated at 37 °C for 24 h, and then colonies were counted. No bacterial colonies would be observed if the tested material concentration is bactericidal. The results are shown in Table 1.

3.8. Antifungal Activity by Disk Diffusion Method. The in vitro antifungal properties of CdTe-κC-g-PDMA-4 have been evaluated against S. Sclerotiorum by disk diffusion technique (Figure 11). After 48 h, no inhibitory effect was observed and no difference was observed between control sample and QDs; and fungus covered the entire surface of PDA plates.

3.9. Cytotoxicity of QDs. To evaluate the effect of CdTe-κC-g-PDMA-4 on mammalian cells, the MTT assay was performed. The MTT cell proliferation assay is a colorimetric assay system that measures the reduction of a tetrazolium component (MTT) into an insoluble formazan product by the mitochondria of viable cells. After incubation of the cells with the MTT reagent for approximately 2−4 h, a detergent solution is added to lyse the cells and solubilize the colored crystals. The amount of color produced is directly proportional to the number

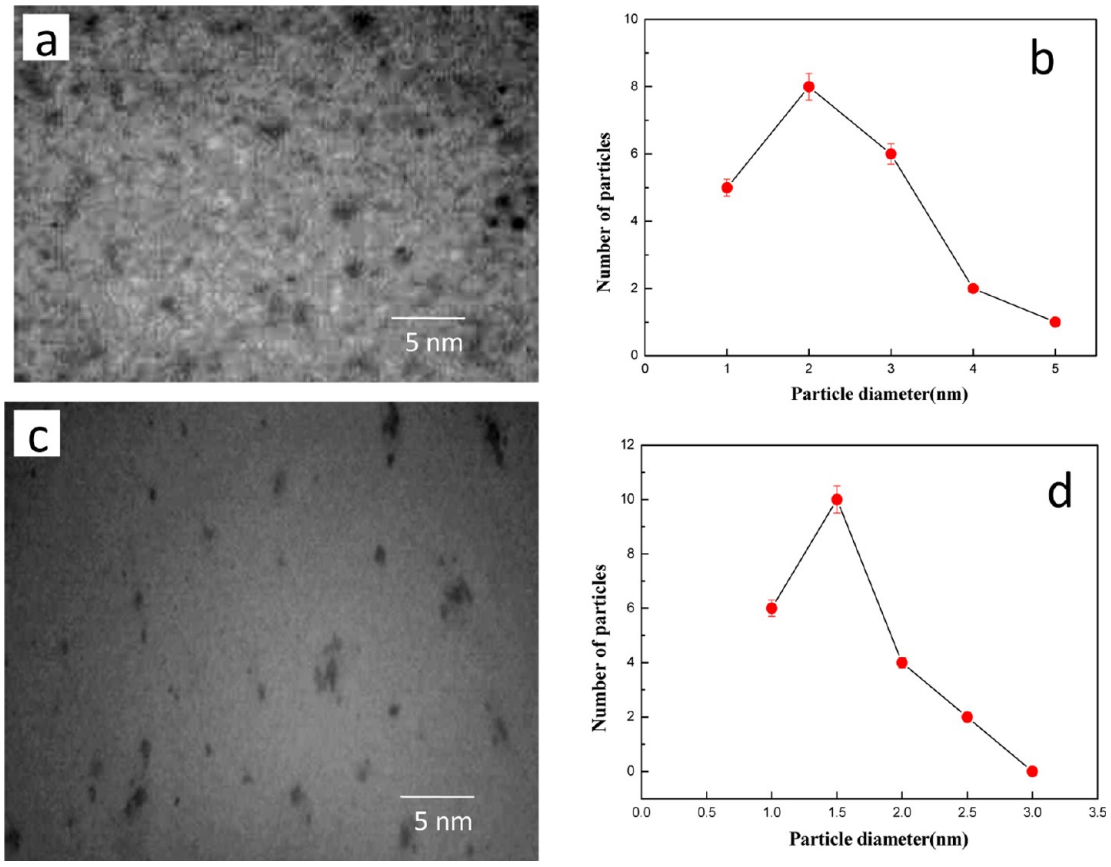

Figure 9. TEM images and the particle size histogram of the (a and b) CdTe-TGA QDs and (c and d) CdTe-κC-g-PDMA-4 QDs.

Scheme 3. Proposed Mechanism for Preparation of CdTe-κC-g-PDMA QDs

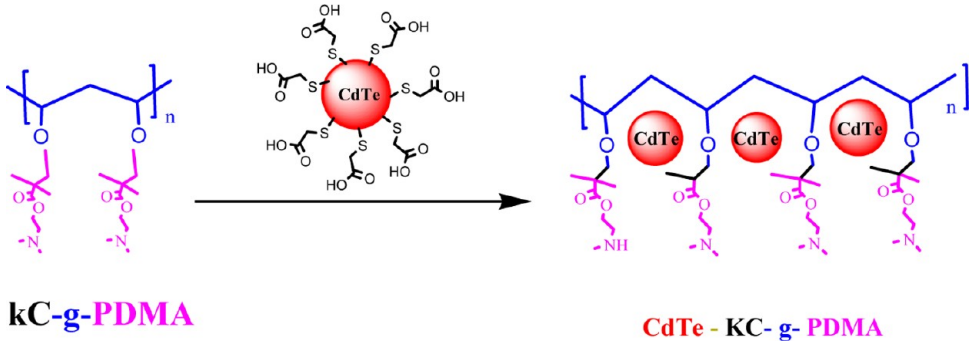

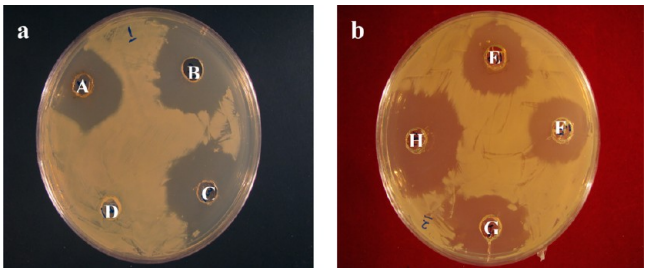

Figure 10. Antibacterial activity of CdTe-κC-g-PDMA-4 QDs against (a) gram-negative *E. coli* and (b) gram-positive *B. licheniformis* by agar diffusion method. A, B, and C are 4, 6, and 8 μg/mL of CdTe-κC-g-PDMA-4 QDs, respectively; and D is distilled water as a negative control. E, F, and G are 4, 6, and 8 μg/mL of CdTe-κC-g-PDMA-4 QDs, respectively; and H is ampicillin as a positive control.

Table 1. MIC and MBC of CdTe-κC-g-PDMA-4 against Two Different Bacteria

Sample	*E. coli*	B. licheniformis
MIC (μg/mL)	7	8
MBC (μg/mL)	9	10

of viable cells. The human bladder epithelial cell line HTB 5637 was grown in RPMI 1640 supplemented with 10% fetal bovine serum. In each well of 96 ELISA plate, 5000 cell was cultivated and different concentration of QDs were added to cells. After 30 h, the MTT assay was done and as one can see from Figure 12, no cytotoxicity was observed. It was observed that the CdTe-κC-g-PDMA is nontoxic even at very high concentration, which is probably because of the fact that the κC-g-PDMA effectively protects the release of cadmium ions (Figure 13). In this regard,

dx.doi.org/10.1021/am300566u | *ACS Appl. Mater. Interfaces* 2012, 4, 3517−3525

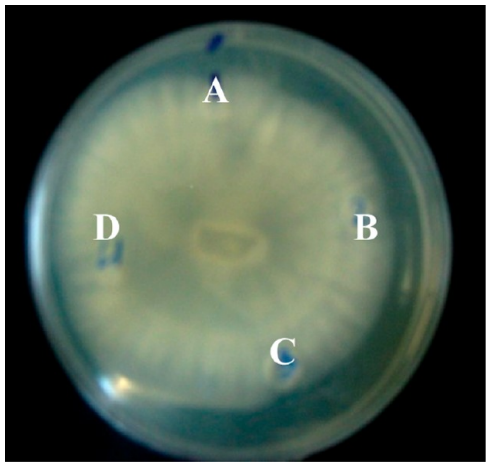

Figure 11. Antifungal effect of different concentration (A = 4, B = 6, and C = 8 μg/mL) of CdTe-κC-g-PDMA-4. D is distilled water as a control sample.

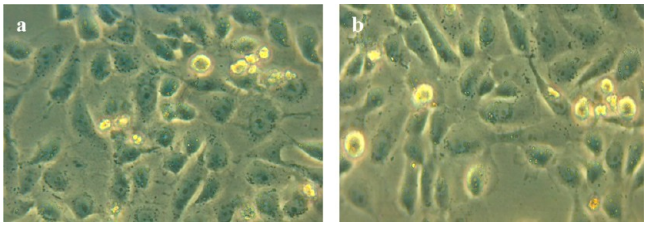

Figure 12. Cytotoxicity test of (a) inverted microscopic photo of 5637 cell line before treatment, and (b) 30 h after treatment with CdTe-κC-g-PDMA-4 QDs (magnification 200×).

the entitled QDs can be regarded as a good candidate for further biological applications.

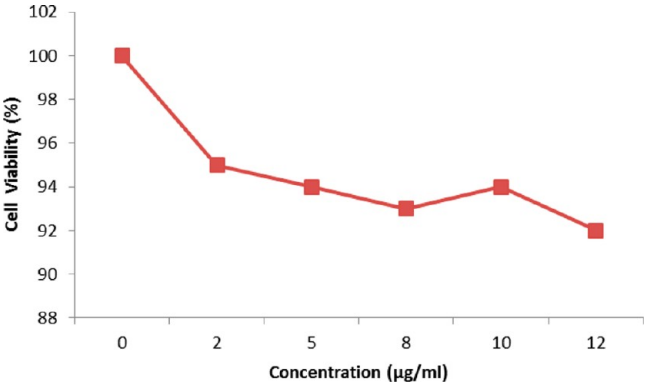

Figure 13. Cytotoxicity of CdTe-κC-g-PDMA with different concentrations on HTB 5637 cell line (Viability of HTB 5637 cells after treatment with QDs in DMEM/F12 medium at 37 °C in the humidified atmosphere with 5% CO2. The cell viability was calculated as a percentage from the viability of the control (untreated) cells. The viability of the control cells was considered 100%).

4. CONCLUSIONS

To sum up, the surface of CdTe QDs was modified by κC-g-PDMA biopolymer. The interaction between κC-g-PDMA and CdTe QDs enhanced the optical properties of QDs. The effects of concentration of DMA monomer, molar ratio of CdTe: κC-g-PDMA, and reaction temperature on the optical properties of CdTe-κC-g-PDMA were investigated. The results showed that the highest FL intensity is related to CdTe-κC-g-PDMA-4 with ratio of κC-g-PDMA-4/CdTe= 1:4 at 25 °C. The TEM images of CdTe QDs showed that the average size of QDs was about 1.7 nm which is in good agreement with the average particle size obtained using UV results. FT-IR and TG characterizations indicated the formation of robust bonding between CdTe QDs and the biopolymeric ligands. Biocompatibility tests showed that the biopolymer modified QDs have not any cytotoxicity, and can be regarded as a good candidate for further biological applications.

AUTHOR INFORMATION

Corresponding Author

*Tel.: +98 281 3336366; fax: +98 281 3344081. E-mail addresse: rezanejad@pnu.ac.ir.

Notes

The authors declare no competing financial interest.

ACKNOWLEDGMENTS

We are grateful to the PNU and INSF for funding this work. The authors also thank Dr. Mohsen Soleymani for very helpful discussion on measuring the quantum yields of QDs.

REFERENCES

(1) Ge, S.; Lu, J.; Ge, L.; Yan, M.; Yu, J. *Spectrochim. Acta, Part A* **2011**, *79*, 1704−1709.
(2) El-sadek, M. S. A.; Nooralden, A. Y.; Babu, S. M.; Palanisamy, P. K. *Opt. Commun.* **2011**, *284*, 2900−2904.
(3) Fan, X.; Peng, J.; Yan, S.; Wang, L.; He, Y. *J. Lumin.* **2011**, *131*, 2230−2236.
(4) Peng, J.; Liu, S.; Wang, L.; He, Y. *Spectrochim. Acta, Part A* **2010**, *75*, 1571−1576.
(5) Wang, J.; Han, H. *J. Colloid Interface Sci.* **2010**, *351*, 83−87.
(6) Jhonsi, M. A.; Renganathan, R. *J. Colloid Interface Sci.* **2010**, *344*, 596−602.
(7) Li, M.; Xu, X.; Tang, Y.; Guo, Z.; Zhang, H.; Zhang, H.; Yang, B. *J. Colloid Interface Sci.* **2010**, *346*, 330−336.
(8) Han, J.; Spanheimer, C.; Haindl, G.; Fu, G.; Krishnakumar, V.; Schaffner, J.; Fan, C.; Zhao, K.; Klein, A.; Jaegermann, W. *Sol. Energy Mater. Sol. Cells* **2011**, *95*, 816−820.
(9) Jie, J.; Zhang, W.; Bello, I.; Lee, C.; Lee, S. *Nano Today* **2010**, *5*, 313−336.
(10) Chen, L.; Qi, Z.; Chen, R.; Li, Y.; Liu, S. *Clin. Chim. Acta* **2010**, *411*, 1969−1975.
(11) Gaponik, N.; Talapin, D. V.; Rogach, A. L.; Hoppe, K.; Shevchenko, E. V.; Kornowski, A.; Eychmueller, A.; Weller, H. *J. Phys. Chem. B* **2002**, *106*, 7177−7185.
(12) Zhavnerko, G. K.; Agabekov, V. E.; Gallyamov, M. O.; Yaminsky, I. V.; Rogach, A. L. *Colloids Surf. A* **2002**, *202*, 233−241.
(13) Mandal, A.; Tamai, N. *Chem. Phys. Lett.* **2011**, *507*, 248−252.
(14) El-sadek, M. S. A.; Kumar, J. R.; Babu, S. M. *Curr. Appl. Phys.* **2010**, *10*, 317−322.
(15) Tian, J.; Liu, R.; Zhao, Y.; Xu, Q.; Zhao, S. *J. Colloid Interface Sci.* **2009**, *336*, 504−509.
(16) Shang, Q.; Wang, H.; Yu, H.; Shan, G.; Yan, R. *Colloids Surf. A* **2007**, *294*, 86−91.
(17) Jhonsi, M. A.; Renganathan, R. *J. Colloid Interface Sci.* **2010**, *344*, 596−602.
(18) Feng, X.; Shang, Q.; Liu, H.; Wang, W.; Wang, Z.; Liu, J. *J. Lumin.* **2010**, *130*, 648−653.
(19) Peng, H.; Zhang, L.; Soeller, C.; Travas-Sejdic, J. *J. Lumin.* **2007**, *127*, 721−726.
(20) Li, J.; Wang, L.; Zhao, K.; Li, D.; Li, J.; Bai, Y.; Li, T. *Colloids Surf. A* **2005**, *257*−*258*, 329−332.

(21) Dunstan, D. E.; Chen, Y.; Liao, M. L.; Salvatore, R.; Boger, D. V.; Prica, M. *Food Hydrocolloids* **2001**, *15*, 475−484.
(22) Hemar, Y.; Hall, C. E.; Munro, P. A.; Singh, H. *Int. Dairy J.* **2002**, *12*, 371−381.
(23) Sedlmeyer, F.; Daimer, K.; Rademacher, B; Kulozik, U. *Colloids Surf. B* **2003**, *31*, 13−20.
(24) Alexander, M.; Dalgleish, D. G. *Food Hydrocolloids* **2007**, *21*, 128−136.
(25) Verbeken, D.; Bael, K.; Thas, O.; Dewettinck, K. *Int. Dairy J.* **2006**, *16*, 482−488.
(26) Bardajee, G. R.; Hooshyar, Z.; Rostami, I. *Colloids Surf. B* **2011**, *88*, 202−207.
(27) Bardajee, G. R.; Hooshyar, Z. *Colloids Surf. A* **2011**, *387*, 92−98.
(28) Bardajee, G. R.; Hooshyar, Z.; Pourhasan, Y. *Int. J. Spectrosc* **2011**, *2011*, 1−20.
(29) Yu, W. W.; Qu, L.; Guo, W.; Peng, X. *Chem. Mater.* **2003**, *15*, 2854−2860.
(30) Lin, W.; Fritz, K.; Guerin, G.; Bardajee, G. R.; Hinds, S.; Sukhovatkin, V.; Sargent, E. H.; Scholes, G. D.; Winnik, M. A. *Langmuir* **2008**, *24*, 8215−8219.
(31) Crosby, G. A.; Demas, J. N. *J. Phys. Chem.* **1971**, *75*, 991−1024. (b) www.jobinyvon.co.uk/jy/fluorescence/applications/quantumyieldstrad.pdf.